Batteries & Supercaps

Research Article
doi.org/10.1002/batt.202500008

Chemistry Europe
European Chemical Societies Publishing

www.batteries-supercaps.org

Increasing Redox Potential of Pyromellitic Diimide by Chemical Modifications: Toward High-Voltage Organic Positive Electrode for Lithium Battery

Valentin Gouget, Pierre-Alain Bayle, Amélie Kochem, Nicolas Leconte, Laurent Bernard, Lionel Picard, and Thibaut Gutel*

Lithium batteries are considered as the most promising electricity storage solution to support the energy transition but still suffer for cost and sustainable issues related to the use of transition metal-based electrode materials. Due to their reduced environmental footprint and low cost, organic active materials such as carbonyl family (quinone, anhydride, diimide) are some interesting candidates to replace them but electrochemical performances in particular redox potential have to be increased in order to become a viable alternative. Here benefiting from tunability of organic structure and guided by rational design rules based on Hammett theory, new strategies are proposed to increase the redox potential of molecular diimide by introducing electron-withdrawing groups such as bromine, cyano, or nitro groups. This work can be considered as a first step to develop some competitive positive electrodes materials based on organic molecules or polymers using diimide derivatives.

1. Introduction

The transition from fossil fuels to more environmental-friendly energy sources requires a massive implementation of efficient electrification solutions, especially in tense sectors such as transportation and industrial processes, making urgent the fast development of energy storage systems. Moreover portable electronics are omnipresent in our everyday life and require batteries with ever higher energy densities. Due to their high electrochemical performances, lithium-ion batteries (LIBs) have been identified as the most promising solution to store electricity for various applications but their electrodes are mainly based on the use of critical raw materials (CRMs),[1] especially transition metals such as cobalt and nickel. Finally extraction from geological ores and energy-consuming transformations processes make the supply chain of these inorganic materials expensive and poorly renewable, thus highlighting the severe environmental footprint of LIB technologies.

Since the pioneering work of Armand et al. in 2009,[2] many redox active groups such as nitroxyde, organosulfide, carbonyls,…[3,4] have been reported showing that organic electrode materials (OEM) represent a seducing alternative to replace CRM, as they are synthesized from sustainable precursors using green chemistry processes. Furthermore, the inherent versatility of organic synthesis allows for a precise tuning of their electrochemical properties, enhancing their performance in various applications including lithium batteries. However, although many reported OEMs feature high and competitive specific capacities (>150 mAh g^{-1}) compared to their inorganic counterparts, they still suffer from important drawbacks such as solubility issues, weak electronic conductivities, or too low redox potentials in order to target their use as positive electrode materials.

First reported by Poizot et al. as discrete molecules[5] but popularized in polymer forms by Song,[6] diimide and polyimide derivatives respectively are very interesting redox compounds due to their intrinsic high thermal and chemical stabilities[7] and their multielectron electrochemical processes leading to high specific capacity. Moreover, as a member of carbonyl-based electrode materials like quinones, anhydrides, and carboxylates, their n-type electrochemical mechanism is compatible with cation–ion configuration using Li^+, Na^+, K^+ but also Mg^{2+}[8] or Ca^{2+}[9] counterions. However diimide redox potentials (2–2.5 V vs. Li^+/Li against some target values comprised between 3 and 4 V vs. Li^+/Li) are still too low to be used as efficient positive electrode material even if recent examples of full organic cells using polyimides have been reported in the literature.[10,11]

The diversity of organic redox compounds is a wonderful playground for organic chemists and electrochemists as illustrated by numerous recent reviews on the topics.[3,4,12,13] Nevertheless some guidelines are required to properly design

V. Gouget, L. Bernard, L. Picard, T. Gutel
CEA, Liten, DEHT
University Grenoble Alpes
F-38054 Grenoble, France
E-mail: thibaut.gutel@cea.fr

P.-A. Bayle, A. Kochem
CEA, CNRS, IRIG, MEM
University Grenoble Alpes
F-38054 Grenoble, France

N. Leconte
Département de Chimie Moléculaire
University Grenoble Alpes
F-38000 Grenoble, France

Supporting information for this article is available on the WWW under https://doi.org/10.1002/batt.202500008

Research Article
doi.org/10.1002/batt.202500008
Chemistry Europe
European Chemical Societies Publishing

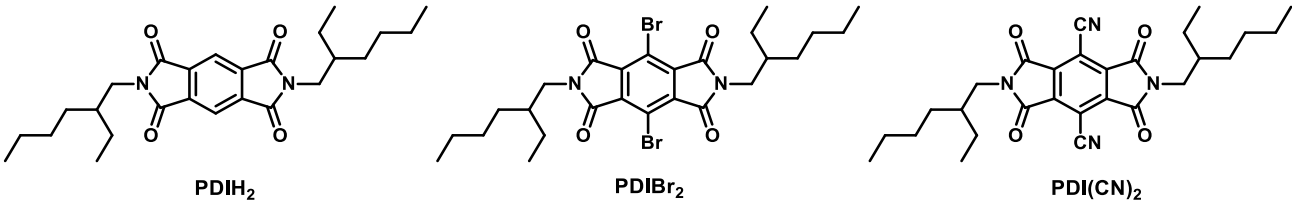

Figure 1. Structures of pyromellitic diimide ($PDIX_2$) functionalized with hydrogen (X = H), bromide (X = Br) and cyanide (X = CN).

new structures and anticipate the electrochemical properties of targeted molecules. Since the initial report by Hansch et al.[14] that describes the behavior of benzoic acids (Figure S1, Supporting Information), the Hammett theory stands among the most well-established easy-to-use theoretical tools and is continuously and successfully exploited to rationalize electronic effects of substituents in aromatics. Accordingly we envisioned that the Hammett theory could be a reliable mean to predict the electrochemical properties of an OEM by correlating the nature of substituents and the redox potential. To demonstrate the interest of this approach, the case of diimide derivatives has been chosen.

Herein, we report a novel synthetic strategy driven by the Hammett parameter to functionalize the pyromellitic diimide (PDI) backbone with electron-withdrawing groups (EWGs), such as bromide and cyanide (**Figure 1**). This approach aims to enhance the redox potential of $PDIH_2$ to $PDIBr_2$ and finally to $PDI(CN)_2$.

2. Results and Discussion

2.1. Prediction Based on Hammett Parameter

Hammett factors have been originally introduced in order to quantify the electronic effects of various meta substituents on benzoic acids. With the pyromellitic diimide backbone in hand, we envisioned that the Hammett constants could be helpful for the rational design of a derivative with increased working potentials. Indeed, even if it is not possible to precisely predict the value of redox potential of the final product, the substitution of H by strong EWGs will increase it proportionally to their inductive power (**Figure 2**).

According to Hammett theory, cyano (–CN), nitro ($–NO_2$), trifluorosulfonyl ($–SO_2CF_3$), and trimethylammonium ($–NMe_3^+$) are among the strongest EWGs. Considering the molecular weight of trifluoromethanesulfonyl (133 g mol^{-1}) which would be detrimental for specific capacity of the corresponding structure, this substituent was excluded from our study. H-substituted pyromellitic diimide ($PDIH_2$) was studied as reference and the dibromo derivative ($PDIBr_2$) was prepared as intermediate for the introduction of functional groups.

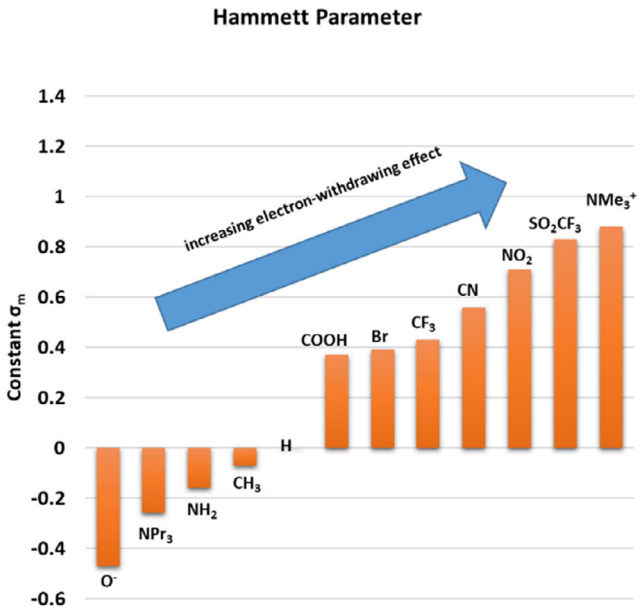

Figure 2. Hammett parameters (σ_m) for various substituents in meta position reported by Hansch et al.[14] H is fixed at 0.

2.2. Synthesis

The general syntheses of the PDI derivatives start from their corresponding dianhydride precursors and are depicted in **Figure 3**.

By anticipation of the next synthetic steps as well as the subsequent electrochemical study in solution, we've chosen to prepare soluble PDI derivatives. This was successfully achieved by reacting commercially available anhydrides **1** and **2** with chiral 2-ethylhexylamine. After 3 h in refluxing acetic acid, the desired $PDIH_2$ and $PDIBr_2$ were isolated in 95% and 98% yields, respectively.

In our search for a PDI derivative with optimized electrochemical performances, we initially directed our efforts to the functionalization with nitrogenated substituents, that is, nitro and trialkylammonium. The preparation of $PDI(NO_2)_2$ was thus investigated, especially as the dinitro compound could be also a suitable precursor for the diammonium species $PDI(NR_3^+)_2$ (Figure 3). Several nitration conditions were screened to get $PDI(NO_2)_2$ from $PDIH_2$. Unfortunately, neither conventional nitration procedures (concentrated nitric acid in sulfuric or acetic acid) nor catalytic alternatives (concentrated nitric acid in dichloromethane with Cerium Ammonium Nitrate "CAN" as additive) afforded the desired compound. Noteworthily, whatever the method used, the careful NMR monitoring never evidenced any traces of the target $PDI(NO_2)_2$ (Figure S2, Supporting Information).

We next turned our attention toward another promising candidate: the dicyano $PDI(CN)_2$. Recent developments in

Research Article
doi.org/10.1002/batt.202500008
Chemistry Europe
European Chemical Societies Publishing

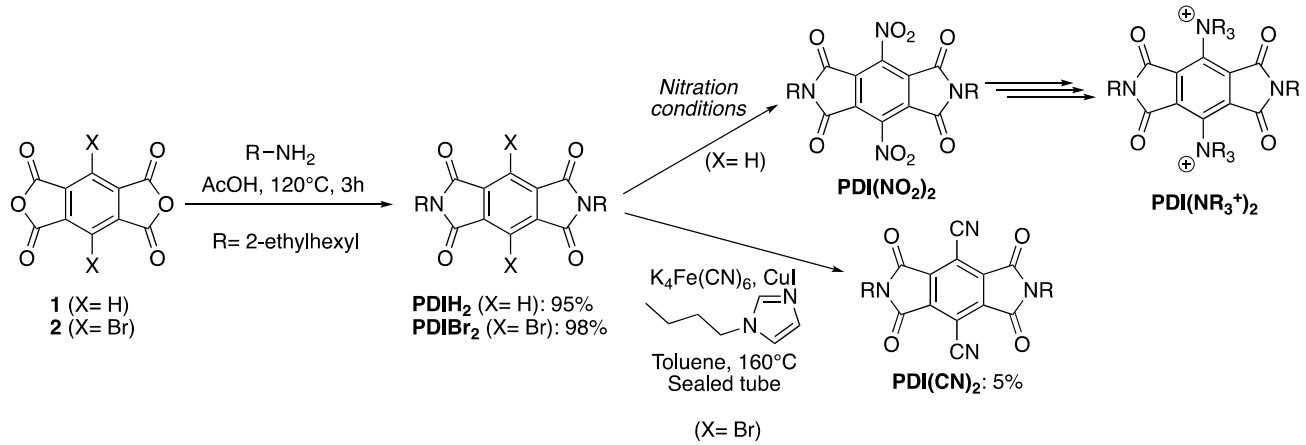

Figure 3. Synthetic routes of the $PDIX_2$ derivatives (X = H, Br, CN).

cyanation procedures led us to consider the Cu-catalyzed reaction described by Beller et al.[15,16] In this work, benzonitriles are obtained from the reaction between haloarenes and $K_4Fe(CN)_6$ under copper(I) catalysis. The strategy is seducing as it overcomes the use highly toxic copper cyanide found in conventional cyanation reactions (Ullman-type mechanism).[17,18] Instead, $K_4Fe(CN)_6$ is a completely nontoxic cyanide source, classically used as a food additive. Adapting Beller's conditions, the CuI-catalyzed cyanation of $PDIBr_2$ in the presence of $K_4Fe(CN)_6$ was carried out (Figure 3). The reaction kinetics was monitored by ^{13}C NMR. Indeed the monoaddition of cyanide moieties of $PDIBr_2$ leads to an easily detected symmetry breaking due to the appearance of new signal in the range of 105–115 ppm attributed to aromatic carbon which fully disappears when the reaction is completed (Figure S3, Supporting Information). Despite a 5% yield and the residual traces of impurity, the dicyano derivative was successfully isolated. The low-but-unoptimized yield is attributed to the partial degradation of the target compound during the reaction.

Before running a further optimization sequence, we were curious to evaluate the electrochemical properties of the three isolated pyromellitic diimide derivatives of general formula $PDIX_2$ (with X = H, Br, CN).

2.3. Electrochemical Behaviors of PDI Derivatives

The cyclic voltammetry (CV) of $PDIX_2$ derivatives was investigated and results are depicted in **Figure 4**. Experiments were run in acetonitrile (ACN) at a 5 mM concentration in $PDIX_2$ and in the presence of tetrabutylammonium perchlorate (TBAP, 0.1 M) as an electrolyte. $Ag/AgNO_3$ has been used a reference electrode and all redox potentials were readjusted versus ferrocene internal standard. Several scan rates have been investigated (Figure S4, Supporting Information). The CV of $PDIH_2$ shows two reversible reductions at $E1_{1/2} = 2.41$ V (vs. Li^+/Li) and $E2_{1/2} = 1.77$ V (vs. Li^+/Li) corresponding to two successive one-electron exchanges, the former leading to the radical anion $[PDIH_2^{\cdot-}]$ and the latter to the dianion structure $[PDIH_2^{2-}]$ as proposed by Renault et al.[5]

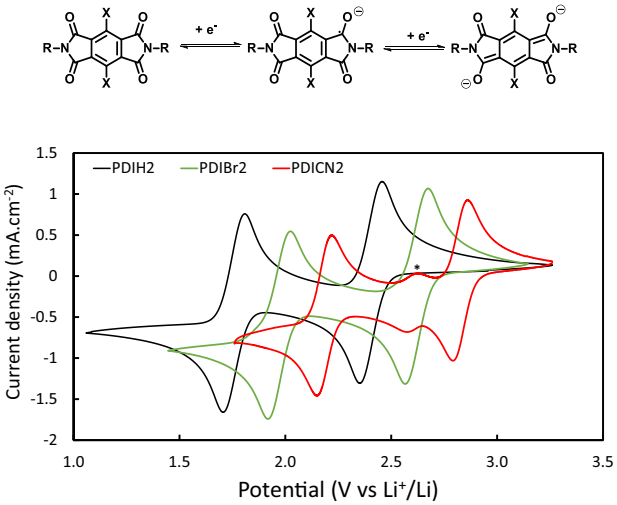

Figure 4. Redox reactions of $PDIX_2$ derivatives and comparison of CV (second cycles) at 100 mV s^{-1} of $PDIH_2$ (black); $PDIBr_2$ (green); and $PDI(CN)_2$ (red) in solution ($C = 5$ mM) in ACN/TBAP 0.1 M with a gold electrode working electrode and platine counter electrode ($\varphi = 3$ mm). $Ag/AgNO_3$ reference electrode was used and the potential was converted to Li^+/Li by substrating 2.5 V. (* this weak signal was attributed to low impurity in $PDI(CN)_2$ product).

As reported in the literature,[19,20] only two carbonyl moieties could be reversibly reduced as further reductions at lower voltages lead to irreversible redox events.

On switching to the $PDIBr_2$ analog, the CV study shows two redox phenomena at significantly higher potentials than those observed with $PDIH_2$. Indeed, the first reduction happens at $E1_{1/2} = 2.62$ V (vs. Li^+/Li) while the second process occurs at $E2_{1/2} = 1.98$ V (vs. Li^+/Li). It is noteworthy that replacing the aromatic H atoms by bromine atoms didn't affect the reversibility of the redox exchanges. In contrast, the increase in potentials is striking and demonstrates the strong inductive effect of bromine atoms compared to hydrogen with a gain of about 210 mV on the mean voltage. Surprisingly the electron-withdrawing inductive effect of the bromine atoms prevails over the electron-donating mesomeric effect, presumably because bromines are grafted symmetrically.

Research Article
doi.org/10.1002/batt.202500008
Chemistry Europe
European Chemical Societies Publishing

We next examined the properties of the dicyano compound $PDI(CN)_2$. On the CV experiment, two reversible redox events are still detected, indicating that the PDI moiety retains its redox active character after the introduction of cyano substituents. Satisfyingly, the one-electron changes occur at even more important potentials than those noted above, with the first reduction reaching $E1_{1/2} = 2.83$ V (vs. Li^+/Li) and the second being located at $E2_{1/2} = 2.19$ V (vs. Li^+/Li). The voltage increase is about 420 mV in comparison with $PDIH_2$.

The CV measurements were conducted at several scan rates and diffusion coefficients of $PDIX_2$ in acetonitrile solution were calculated using the Randles–Sevcik equation (Figure S5, Supporting Information). As expected, the lower the steric hindrance, the higher the diffusion coefficient with $PDIH_2$ (8.53×10^{-6} cm^2 s^{-1}) being more mobile than $PDIBr_2$ (7.05×10^{-6} cm^2 s^{-1}) and $PDI(CN)_2$ (5.71×10^{-6} cm^2 s^{-1}). As current is proportional to local concentration of redox active species, it could explained that its intensity decreases from $PDHI_2$ to $PDIBr_2$ and $PDI(CN)_2$.

As the goal of our work was to demonstrate that a rational design of high-voltage OEM is possible and to illustrate our molecular engineering strategy on pyromellitic diimide backbone, the use of soluble derivatives was mandatory to perform efficient chemical modifications, careful physicochemical and electrochemical characterizations. Consequently we anticipate that electrochemical performances in solid-state electrode will be very poor due to solubility issues of active material into electrolyte of lithium battery. Therefore we decided to not test them in this configuration before to implement strategies to suppress the dissolution such as the preparation of corresponding insoluble polymers or salts.

The good compromise between the strong electron-withdrawing ability and a relatively low molecular mass in comparison with other EWGs (CF_3, NO_2, SO_2CF_3, NR_3^+) makes the cyano function particularly adapted to the design of a redox active material. Our approach confirms the strong inductive effect of cyano group. These benefits have been previously observed in the case of other n-type redox materials such as quinone or diimides. Indeed, Jewoski et al. demonstrated an increase of 300 mV of the redox potential by replacing *o*-benzoquinone by 4-cyano-*o*-benzoquinone.[21] The effect is even more impressive in the case of diimide. Kumar et al. demonstrated a gain of about 850–900 mV when switching from naphthalenediimide to tetracyanonaphthalenedimide.[22] Seifert et al. observed a gap of 800 mV between perylenediimide derivative and its tetracyano analog and were able to prepare an air-stable dianion salt.[23] This last development paves the way for building lithium cell in metal-ion configuration using reduced state and lithium-containing n-type OEM for positive electrode.

2.4. Correlation of Redox Potential with Hammett Parameters

Considering $PDIH_2$ as reference for the Hammett parameter scale (zero value), it is possible to establish a linear correlation between the redox potentials of $PDIBr_2$ and $PDI(CN)_2$ and the Hammett parameter ($\sigma_m(H) = 0$; $\sigma_m(Br) = 0.39$; $\sigma_m(CN) = 0.56$) (**Figure 5**). This result is consistent with the literature[20,24,25] and enables to predict the effect of various substituents on the redox potential of these types of organic compounds.

2.5. Correlation of Redox Potential with NMR Chemical Shifts

Nuclear magnetic resonance is a powerful tool to investigate chemical environment of specific nucleus such as hydrogen or carbon. In our work, the influence of the introduction of EWG onto diimide backbone on the chemical shifts of ^{13}C of carbonyl moieties has been studied. In agreement with the literature,[26] ^{13}C chemical shifts attributed to C = O of $PDIX_2$ are well correlated with Hammett parameter of various substituents (X = H, Br, and CN). Indeed the ^{13}C NMR signals are progressively unshielded as a consequence of electronic effects of each atoms/functions (H < Br < CN). Finally it is possible to make a direct correlation between the redox potential of $PDIX_2$ and the ^{13}C chemical shifts of carbonyl as shown in **Figure 6**. This approach demonstrates that ^{13}C NMR can be used as efficient probe to predict the working potential of redox molecule and it represents a simple and nondestructive way to anticipate electrochemical behaviors of new OEM.

2.6. Quantum Chemistry Calculations

The geometry of the neutral, one-, and two-electron reduced $PDIX_2$ molecules were computed using the ORCA package.[27,28] Geometry optimizations were performed with an efficient composite electronic structure method termed r2SCAN-3c[29] and solvent (acetonitrile) effects were taken into account in quantum chemical calculations using the conductor-like polarizable continuum model (CPCM).[30] The neutral and two-electron reduced species were considered in their diamagnetic closed shell state while the one-electron reduced species were considered in their radical state. The PDI core structures adopt a planar geometry for three redox states but ethylhexylamine substituents prevent the perfect π–π stacking improving the solubility of these products. The highest occupied molecular orbitals (HOMOs) and lowest unoccupied molecular orbitals (LUMOs) of the neutral $PDIX_2$

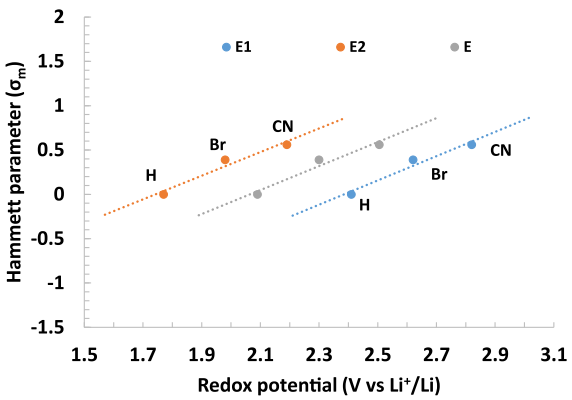

Figure 5. Correlation of Hammett parameter and redox potentials of $PDIH_2$, $PDIBr_2$, and $PDI(CN)_2$. The mean voltage is represented in gray and the correlations with the two redox phenomena are represented with dashed lines.

Research Article
doi.org/10.1002/batt.202500008
Chemistry Europe
European Chemical Societies Publishing

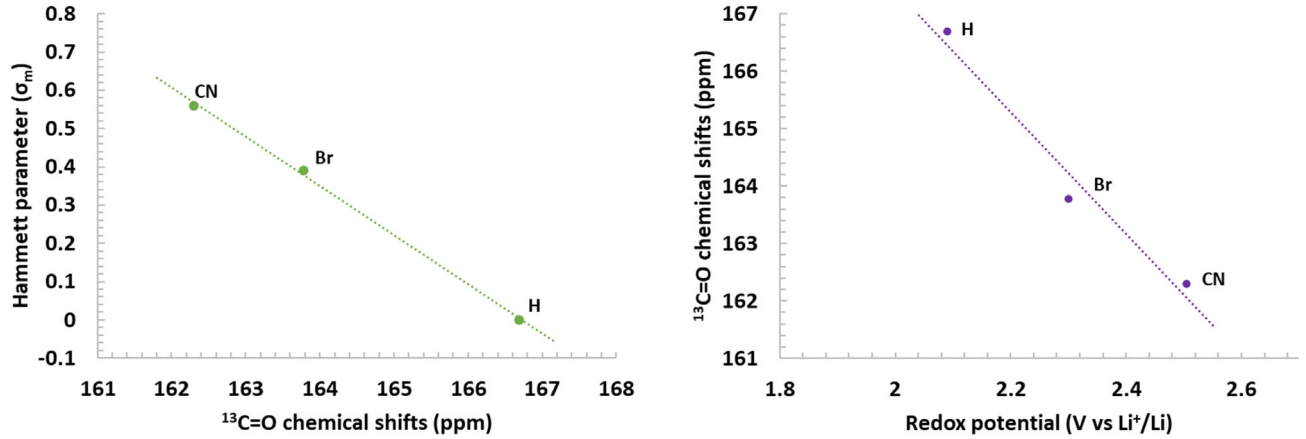

Figure 6. Correlation of ^{13}C chemical shifts of carbonyl group of $PDIX_2$ with (left) Hammett parameter of the substituent and (right) with redox potential of the first reduction (X = H; Br or CN).

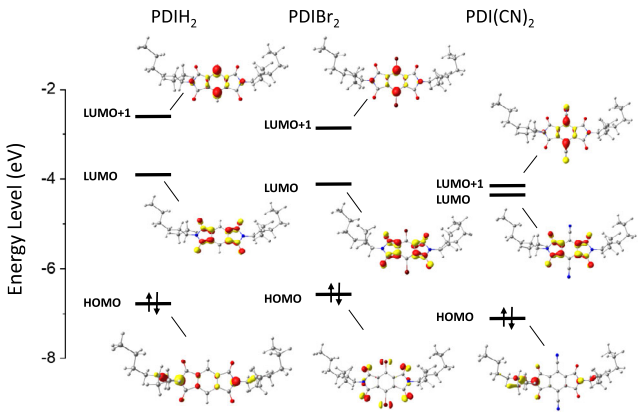

Figure 7. Density functional theory-calculated frontier orbitals of $PDIX_2$ molecules. The HOMO and LUMOs of $PDIX_2$ derivatives obtained from calculations using r2scan-3c method. A contour of 0.07 eÅ^{-3} was used for the orbital plot.

derivatives and the influence of the functionalizing groups on the $PDIX_2$ species on the energy of their frontier orbitals are represented in **Figure 7**. The HOMOs of the neutral molecules are mainly located on the diimide functions of the PDI rings, while the LUMOs are mainly located on the two lateral PDIs rings and the LUMO + 1 on the all PDIs cores.

The spin density profiles of the one-electron reduced species $PDIX_2^-$ show that the added electron is located on the carboxyl groups (Figure S6, Supporting Information). As expected the introduction of electron-withdrawing bromide groups induces a decrease of the LUMOs energy. This effect is even more pronounced in the case of cyanide groups. This result qualitatively agrees with the redox potential values determined by CV of various derivatives with a highest mean voltage for $PDI(CN)_2$.

3. Conclusion

Guided by design rules based on Hammett theory, we successfully synthesized and characterized new soluble pyromellitic diimide derivatives functionalized with hydrogen, bromine, and cyano moieties. The new species were studied by electrochemistry in solution showing, as predicted, a strong increase of the redox potential of 210 and 420 mV by introducing two bromines and cyano groups respectively. This evolution was clearly correlated with Hammett parameters confirming that the σ_m constant, originally determined for benzoic acid, is an amazing tool to help organic chemists in particular those who develop organic active materials for positive electrodes of lithium battery. Moreover a strong relationship between redox potentials and ^{13}C NMR chemical shifts was observed offering a very simple opportunity to anticipate the electronic effect of electron-withdrawing substituents. Finally quantum chemistry calculations based on optimized geometries provide some theoretical explanations of the evolution of energy level of HOMO/LUMO orbitals as a function of the nature of substituents. We expect that our approach will help the community to better design high-voltage organic active materials and pave the way for the development of insoluble diimide-based redox molecules or polymers for positive electrodes of lithium battery.

4. Experimental Section

Chemical and Physical Characterizations

All chemicals were purchased from Sigma-Aldrich and were used as received unless otherwise noted. Any derivatives were characterized by liquid-state NMR and IR spectroscopies. Fourier-transform infrared spectroscopy (FTIR) spectra were recorded on Perkin Elmer Spectrum Two. ^{1}H/^{13}C NMR spectra were recorded on a Bruker 400 MHz spectrometer. Chemical shifts (ppm) were referenced to solvent residual peaks.

Synthesis of PDI Derivatives: N,N′-Bis(2-Ethylhexyl) pyromellitic Imide ($PDIH_2$)

Pyromellitic dianhydride (820 mg, 3.65 mmol) was dissolved in glacial acetic acid (100 mL) in a 250 mL round-bottom flask under argon. Subsequently, under stirring, 2-ethylhexylamine (1.23 mL, 7.37 mmol, 2 eq.) was added to the reaction mixture, leading to a pale yellow

solution. The reaction mixture was stirred at reflux (120 °C) for 3 h. After cooling to room temperature (RT), the solvent was removed under reduced pressure. The remaining crude was dissolved in dichloromethane (50 mL) and the resulting solution was washed three times with water and dried over $MgSO_4$. After filtration, the volatiles were removed under reduced pressure and the pale yellow solid was purified by column chromatography on silica gel (Eluent: dichloromethane) to give the pure product as a white solid (1.53 g, 95% yield). IR): ν(cm^{-1}) 2940, 2930, 2859, 1767, 1699, 1394, 1351, 1155, 1052, 944, 730, 620; ^{1}H NMR (400 MHz, $CDCl_3$): δ (ppm) 8.26 (s, 2H), 3.64 (d, $J = 6.9$ Hz, 4 H), 1.85–1.83 (m, 2H), 1.33–1.29 (m, 16H), 0.94–0.88 (m, 12H); ^{13}C NMR (400 MHz, $CDCl_3$,): δ (ppm) 166.7, 137.3, 118.2, 42.6, 38.4, 30.6, 28.6, 24.0, 23.1, 14.1, 10.5 ppm.

Synthesis of PDI Derivatives: N,N′-Bis(2-Ethylhexyl)-3.6-Dibromopyromellitic Imide ($PDIBr_2$)

A similar procedure was used to produce $PDIBr_2$ starting from 3,6-dibromopyromellitic dianhydride (250 mg, 645 μmol) and 2-ethylhexylamine (218 μL, 1.30 mmol, 2.0 eq.). The pure product was isolated as a pale yellow solid (381 mg, 98% yield). IR: ν(cm^{-1}) 2960, 2927, 2856, 1768, 1702, 1434, 1400, 1170, 1087, 1064, 796, 752, 669; ^{1}H NMR (400 MHz, $CDCl_3$): δ (ppm) 3.63 (d, $J = 7.4$ Hz, 4H), 1.85–1.83 (m, 2H), 1.33–1.29 (m, 16H), 0.94–0.88 (m, 12H); ^{13}C NMR (400 MHz, $CDCl_3$): δ (ppm) 163.8, 136.1, 114.1, 42.9, 38.2, 30.5, 28.5, 23.9, 22.9, 14.1, 10.4.

Synthesis of PDI Derivatives: N,N′-Bis(2-Ethylhexyl)-3,6-Dicyanopyromellitic Imide ($PDI(CN)_2$)

Finely ground $K_4[Fe(CN)_6].3H_2O$ was dried at 80 °C under vaccum (<5 mbar) prior to use. Under argon, in a flame-dried sealable tube equipped with a stirring bar, $K_4[Fe(CN)_6]$ (49 mg, 134 μmol, 40%mol), CuI (6.4 mg, 33.42 μmol, 10%mol), n-butylimidazole (83 mg, 688.5 μmol, 2 eq.), $PDIBr_2$ (200 mg, 334 μmol), and toluene (2 mL) were introduced and the mixture was heated at 160 °C under vigorous stirring for 20 h. After cooling to RT, the reaction mixture was diluted in dichloromethane (5 mL) and the insolubles were removed by filtration though a celite pad. The filtrate was washed with deionized water and dried over $MgSO_4$. After filtration, volatiles were removed under reduced pressure and the remaining residue was purified by column chromatography on silica gel (Eluent: cyclohexane/ethyl acetate; 4/1, v:v) to give a pale yellow powder (8 mg, 5% yield). ^{1}H NMR (400 MHz, $CDCl_3$): δ (ppm) 3.71 (d, $J = 7.2$ Hz 4H), 1.90–1.83 (m, 2H), 1.35–1.28 (m, 16H), 0.94–0.91 (m, 12H); ^{13}C NMR (400 MHz, $CDCl_3$): δ (ppm) 162.3, 138.4, 109.3, 105.8, 43.6, 38.4, 30.7, 28.6, 24.0, 23.0, 14.2, 10.4.

Electrochemical Measurements

CV curves were recorded using a Biologic potentiostat. All analytical experiments were conducted under an argon atmosphere (glove box) in a standard three-electrode electrochemical cell. Tetra-*n*-butylammonium perchlorate (TBAP) was used as supporting electrolyte (0.1 M) in acetonitrile (ACN). Au-based working electrode (disk of 3 mm diameter) was polished using diamond paste before each recording and Pt wire was used as counterelectrode. All CVs were recorded using an $AgNO_3$/Ag reference electrode which was recalibrated against ferrocene-based internal standard and whose potential can be converted to Li^+/Li scale by removing 2.50 V (Figure S4, Supporting Information).

Acknowledgements

The authors would like to acknowledge the Agence National de la Recherche (ANR) and the Bundesministerium für Bildung und Forschung (BMBF) for Ph.D. funding awarded to V.G. This work was performed within the framework of MOLIBE Project.

Conflict of Interest

The authors declare no conflict of interest.

Keywords: dimides · lithium batteries · organic electrode materials

[1] European Commission: E. Directorate-General for Internal Market Industry, SMEs, S. Bobba, S. Carrara, J. Huisman, F. Mathieux, C. Pavel, *Critical Raw Materials For Strategic Technologies and Sectors in the EU – A Foresight Study*, Publications Office **2020**.
[2] M. Armand, S. Grugeon, H. Vezin, S. Laruelle, P. Ribière, P. Poizot, J.-M. Tarascon, *Nat. Mater.* **2009**, *8*, 120.
[3] Y. Liang, Z. Tao, J. Chen, *Adv. Energy Mater.* **2012**, *2*, 702.
[4] P. Poizot, J. Gaubicher, S. Renault, L. Dubois, Y. Liang, Y. Yao, *Chem. Rev.* **2020**, *120*, 6490.
[5] S. Renault, J. Geng, F. Dolhem, P. Poizot, *Chem. Commun.* **2011**, *47*, 2414.
[6] Z. Song, H. Zhan, Y. Zhou, *Angew. Chem., Int. Ed.* **2010**, *49*, 8444.
[7] P. Sharma, D. Damien, K. Nagarajan, M. M. Shaijumon, M. Hariharan, *J. Phys. Chem. Lett.* **2013**, *4*, 3192.
[8] T. Bančič, J. Bitenc, K. Pirnat, A. Kopač Lautar, J. Grdadolnik, A. Randon Vitanova, R. Dominko, *J. Power Sources* **2018**, *395*, 25.
[9] O. Lužanin, A. K. Lautar, T. Pavčnik, J. Bitenc, *Mater. Adv.* **2024**, *5*, 642.
[10] H. Banda, D. Damien, K. Nagarajan, M. Hariharan, M. M. Shaijumon, *J. Mater. Chem. A* **2015**, *3*, 10453.
[11] A. Iordache, V. Delhorbe, M. Bardet, L. Dubois, T. Gutel, L. Picard, *ACS Appl. Mater. Interfaces* **2016**, *8*, 22762.
[12] B. Esser, F. Dolhem, M. Becuwe, P. Poizot, A. Vlad, D. Brandell, *J. Power Sources* **2021**, *482*, 228814.
[13] D. Xu, M. Liang, S. Qi, W. Sun, L.-P. Lv, F.-H. Du, B. Wang, S. Chen, Y. Wang, Y. Yu, *ACS Nano* **2021**, *15*, 47.
[14] C. Hansch, A. Leo, R. W. Taft, *Chem. Rev.* **1991**, *91*, 165.
[15] T. Schareina, A. Zapf, M. Beller, *Chem. Commun.* **2004**, 1388.
[16] T. Schareina, A. Zapf, W. Mägerlein, N. Müller, M. Beller, *Chem. - Eur. J.* **2007**, *13*, 6249.
[17] K. W. Rosenmund, E. Struck, *Ber. Dtsch. Chem. Ges. A/B* **1919**, *52*, 1749.
[18] J. V. Braun, G. Manz, *Justus Liebigs Ann. Chem.* **1931**, *488*, 111.
[19] S. Mazur, P. S. Lugg, C. Yarnitzky, *J. Electrochem. Soc.* **1987**, *134*, 346.
[20] A. Viehbeck, M. J. Goldberg, C. A. Kovac, *J. Electrochem. Soc.* **1990**, *137*, 1460.
[21] P. Jeżowski, O. Crosnier, E. Deunf, P. Poizot, F. Béguin, T. Brousse, *Nat. Mater.* **2017**, *17*, 167.
[22] Y. Kumar, S. Kumar, K. Mandal, P. Mukhopadhyay, *Angew. Chem., Int. Ed.* **2018**, *57*, 16318.
[23] S. Seifert, D. Schmidt, F. Würthner, *Chem. Sci.* **2015**, *6*, 1663.
[24] A. A. Adeniyi, T. L. Ngake, J. Conradie, *Electroanalysis* **2020**, *32*, 2659.
[25] Q. Teng, P. S. Ng, J. N. Leung, H. V. Huynh, *Chem. - Eur. J.* **2019**, *25*, 13956.
[26] L. Stievano, F. Tielens, I. Lopes, N. Folliet, C. Gervais, D. Costa, J.-F. Lambert, *Cryst. Growth Des.* **2010**, *10*, 3657.
[27] F. Neese, *WIREs Comput. Mol. Sci.* **2012**, *2*, 73.
[28] F. Neese, *WIREs Comput. Mol. Sci.* **2022**, *12*, e1606.
[29] S. Grimme, A. Hansen, S. Ehlert, J.-M. Mewes, *J. Chem. Phys.* **2021**, *154*, 064103.
[30] M. Garcia-Ratés, F. Neese, *J. Comput. Chem.* **2020**, *41*, 922.

Manuscript received: January 6, 2025
Revised manuscript received: March 14, 2025
Version of record online: March 17, 2025